# Supplementary Information

## K$_x$(C$_2$H$_8$N$_2$)$_y$Fe$_{2-z}$S$_2$: synthesis, phase structure and correlation between K$^+$ intercalation and Fe depletion

Zhongnan Guo ‡[a], Liang Zhou‡[a], Shifeng Jin[b], Bingling Han,[a] Fan Sun,[a] Wenxia Yuan*[a]

*[a] Department of Chemistry, School of Chemistry and Biological Engineering, University of Science and Technology Beijing, Beijing 100083, China.*

*E-mail:wxyuanwz@163.com; Fax:+86-010-62333033; Tel:+86-010-62332221*

*[b] Research & Development Center for Functional Crystals, Beijing National Laboratory for Condensed Matter Physics, Institute of Physics, Chinese Academy of Sciences, Beijing 100190, China.*

*‡ Zhongnan Guo and Liang Zhou contribute equally to this work.*

## Synthesis of FeS precursor

The binary FeS precursor was synthesized by the hydrothermal method described in Ref. 1. 0.025 mol Fe powder and 0.025 mol Na$_2$S·9H$_2$O were placed into a 23 mL Teflon-lined autoclave, and the 60% of the volume was added by deionized water. The autoclave was then closed and heated at 120~140 °C for 6 days, and then the product was filtered and washed with deionized water until the filtrate was colorless. The sample was finally obtained by drying at room temperature and removing the magnetic impurity with a magnet. The FeS precursor was kept in the Ar-filled glove-box before using.

## Dehydration of ethylenediamine

150 g molecular sieve was heated at 300 °C for 12 hours, then kept at 200 °C and added into 450 ml ethylenediamine. After keeping for one day, the ethylenediamine was separated, denoted as one cycle dehydration. In our work, the ethylenediamine after 8 cycles dehydration was used, in order to eliminate the influence of the water during the intercalation (as shown in Fig. S1).
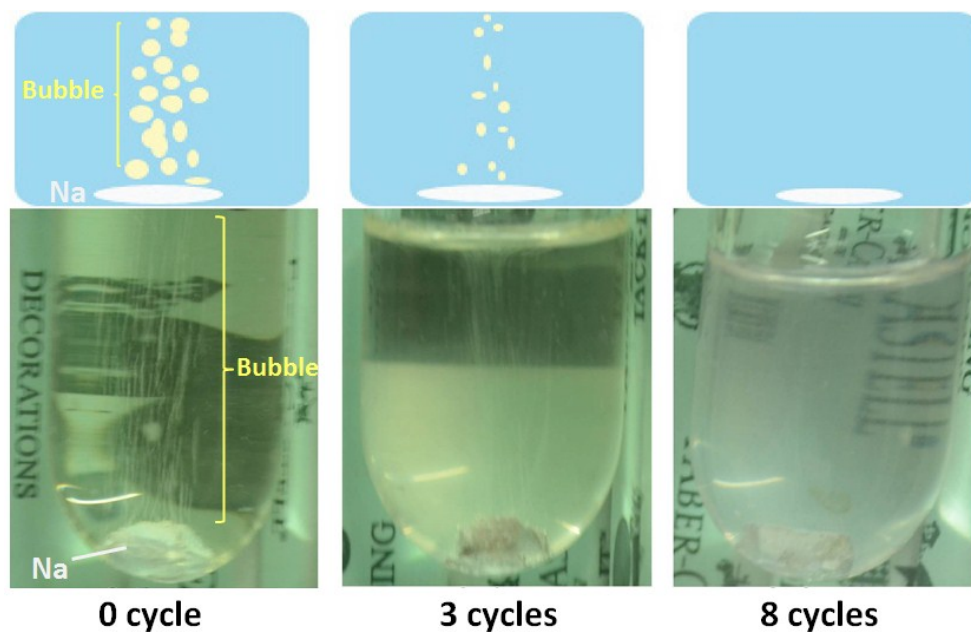
**Fig. S1** Schematic diagram (upper) and photograph (lower) of the alkali metal Na plate in ethylenediamine after different dehydration cycles. As shown in left and middle, the residual water would react with Na, leading to the generation of bubbles. After 8 times dehydration, basically no bubbles could be seen when Na was added.
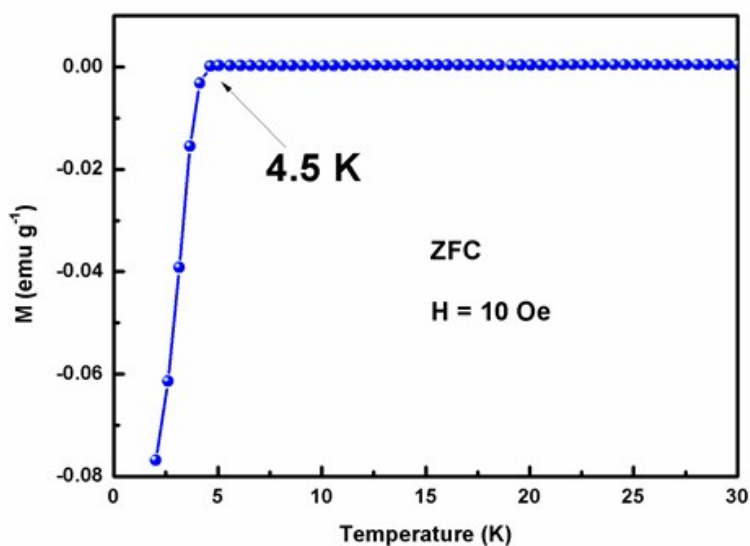


**Fig. S2** Temperature dependence of magnetic susceptibility of binary FeS in ZFC mode, with an applied field of 10 Oe.
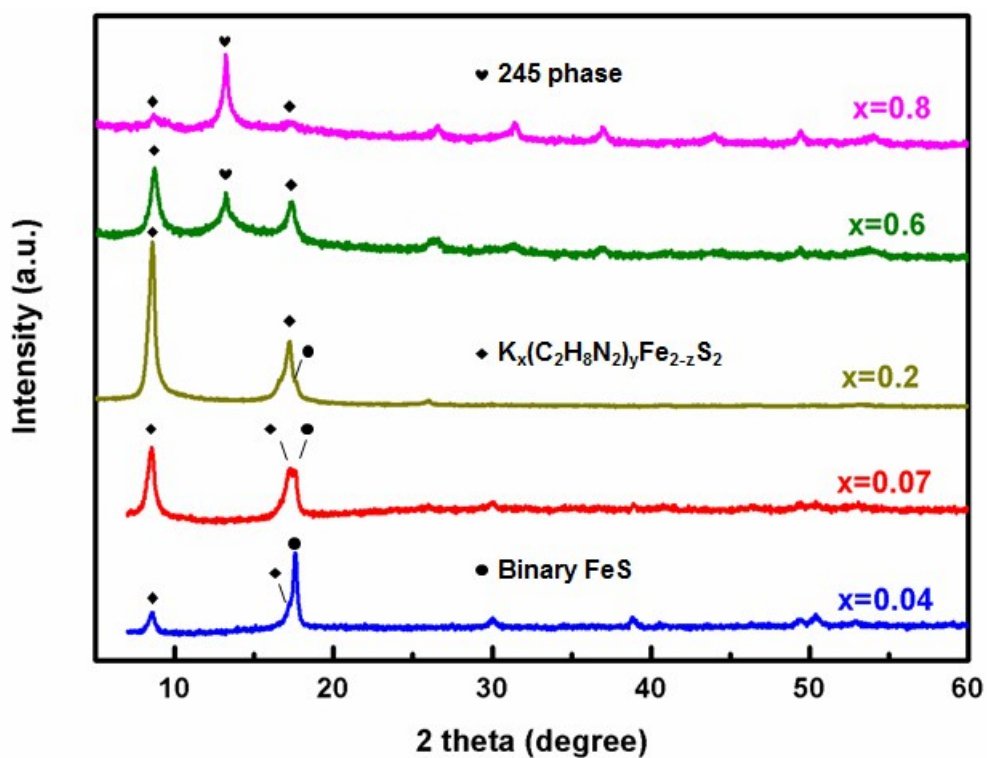
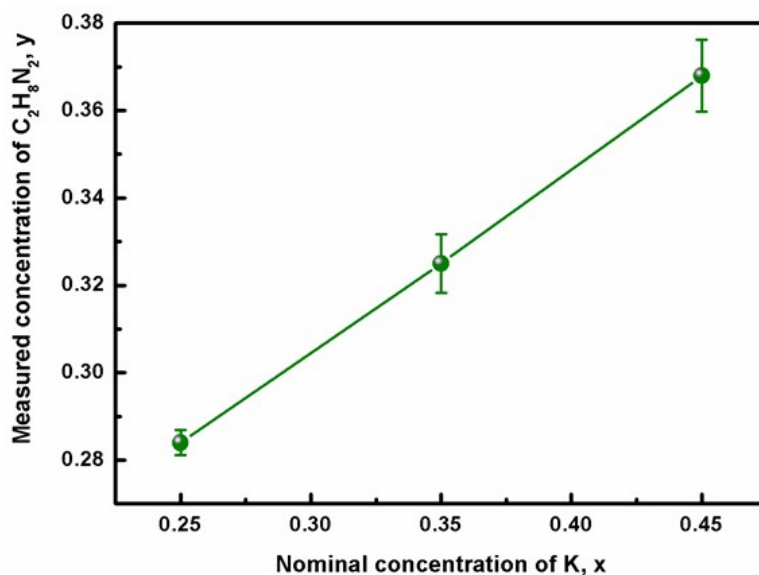**Fig. S3** PXRD patterns of $K_x(C_2H_8N_2)_yFe_{2-z}S_2$ ($x$ = 0.04, 0.07, 0.2, 0.6 and 0.8).



**Fig. S4** The linear dependence of the nominal concentration of K, $x$ and the measured content of the $C_2H_8N_2$ molecule, y.
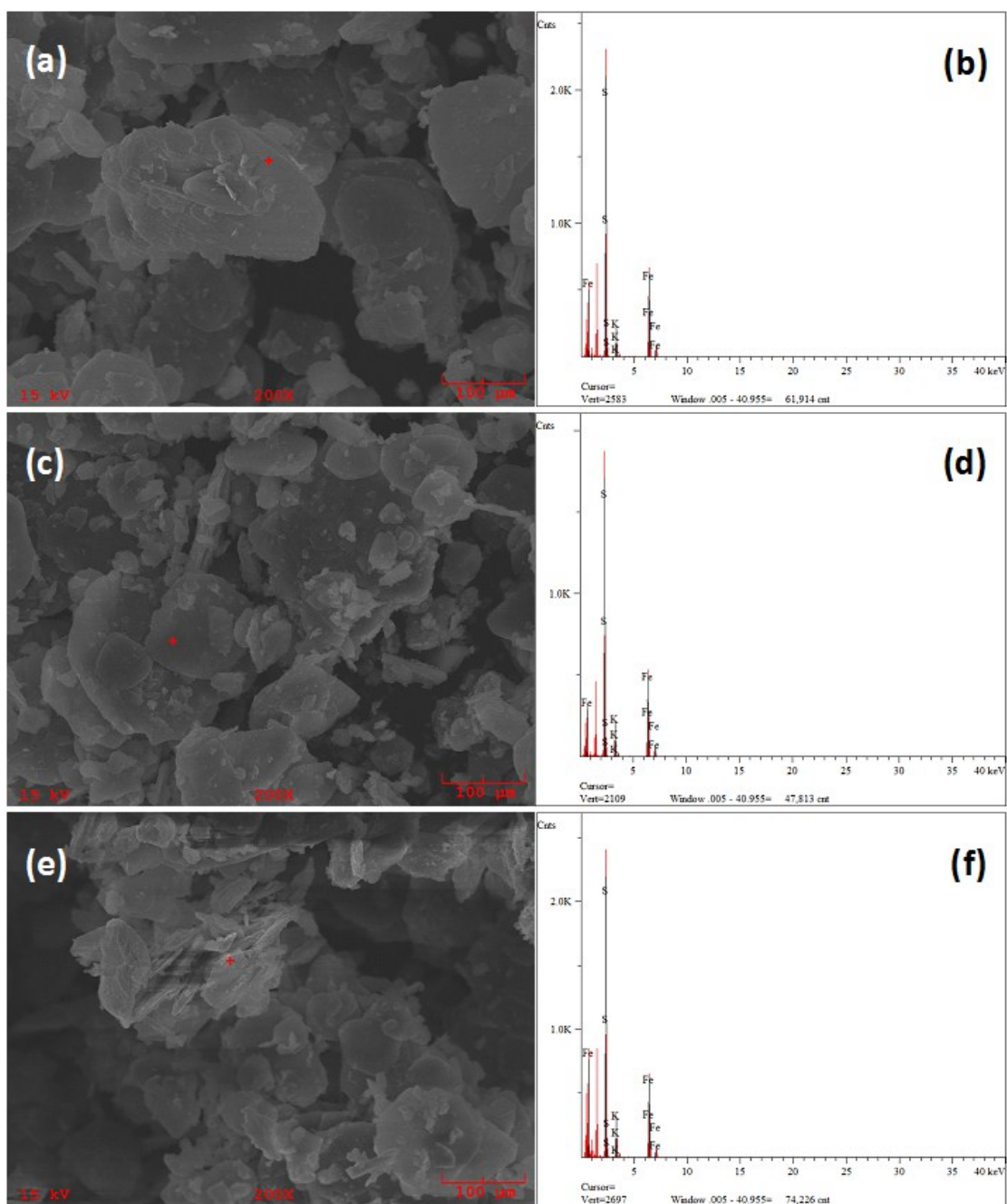
**Fig. S5** The SEM images of $K_x(C_2H_8N_2)_yFe_{2-z}S_2$ with $x$ = (a) 0.25, (c) 0.35 and (e) 0.45, and the EDS patterns of samples with $x$ = (b) 0.25, (d) 0.35 and (f) 0.45.

**Table S1** Elemental compositions of parent FeS ($x = 0$) and $K_x(C_2H_8N_2)_yFe_{2-z}S_2$ with $x = 0.25$, 0.35 and 0.45.

| Nominal $x$ | 1 | 2 | 3 |
|---|---|---|---|
| 0 | $Fe_{1.01(1)}S$ | $Fe_{1.03(2)}S$ | 0 |
| 0.25 | $K_{0.24(1)}(C_2H_8N_2)_yFe_{1.88(1)}S_2$ | $K_{0.23(2)}(C_2H_8N_2)_yFe_{1.93(2)}S_2$ | 0.284(3) |
| 0.35 | $K_{0.31(1)}(C_2H_8N_2)_yFe_{1.83(1)}S_2$ | $K_{0.33(2)}(C_2H_8N_2)_yFe_{1.87(3)}S_2$ | 0.325(7) |
| 0.45 | $K_{0.39(2)}(C_2H_8N_2)_yFe_{1.79(2)}S_2$ | $K_{0.37(3)}(C_2H_8N_2)_yFe_{1.85(3)}S_2$ | 0.368(8) |

Note: 1. Chemical composition from EDS;
2. Chemical composition from ICP-AES.
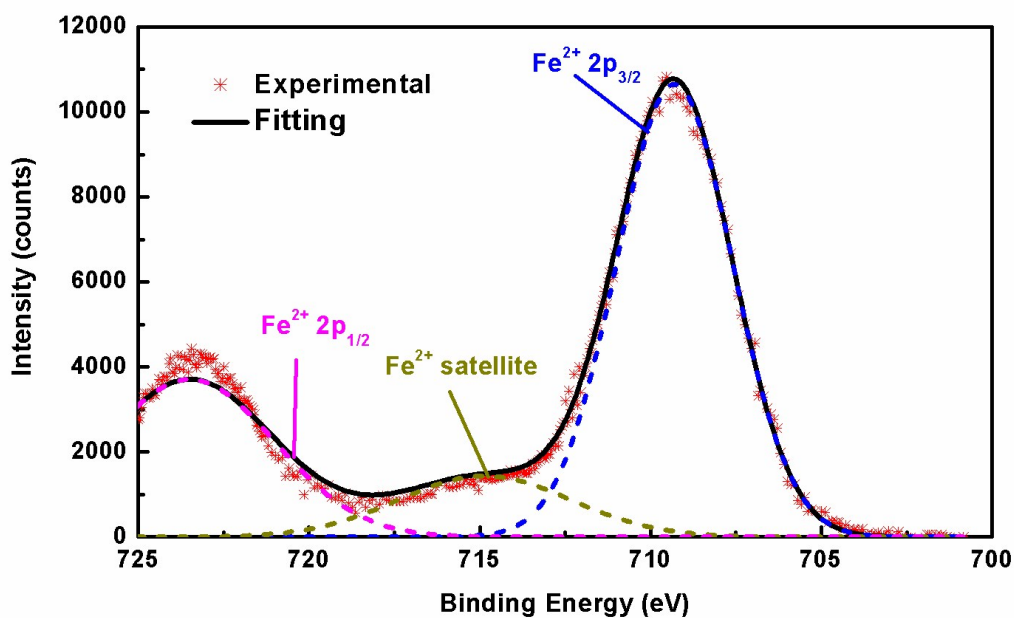3. The $(C_2H_8N_2)$ content, y from the standard micro-Kjedahl method.



**Fig. S6** XPS Fe spectra of binary FeS precursor, showing the single +2 valence.
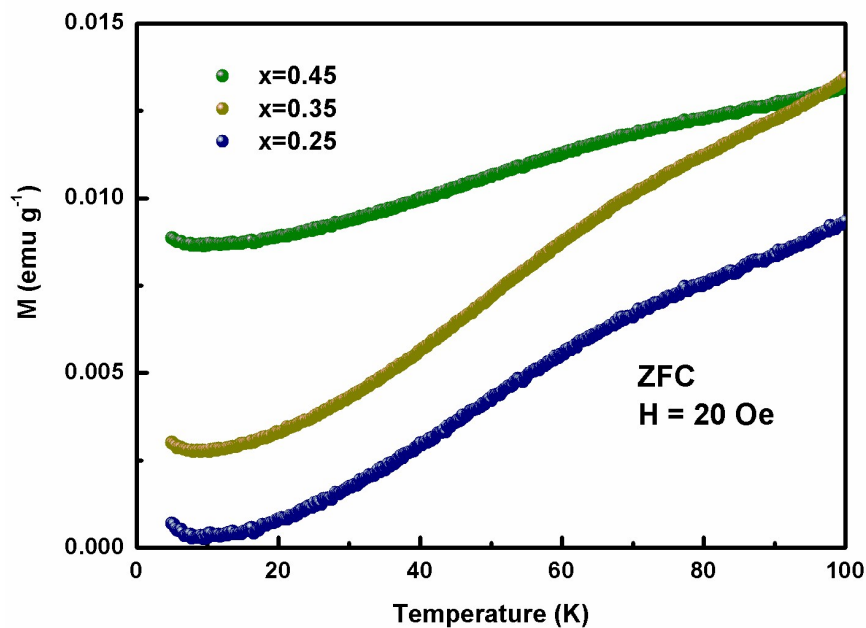
**Fig. S7** Temperature dependence of magnetic susceptibility of $K_x(C_2H_8N_2)_yFe_{2-z}S_2$ with the applied field H = 20 Oe, showing no superconductivity down to 5 K.
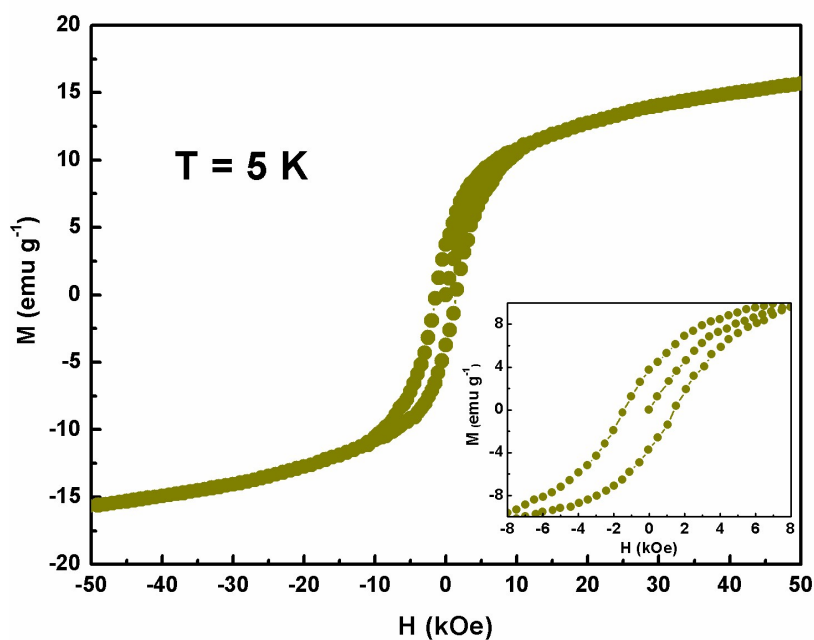


**Fig. S8** Magnetic hysteresis loop of $K_x(C_2H_8N_2)_yFe_{2-z}S_2$ with $x$ = 0.35 at 5 K. Inset shows the enlarged magnetic hysteresis in the field range from -8 to 8 kOe..

## References

1.    X. Lai, H. Zhang, Y. Wang, X. Wang, X. Zhang, J. Lin and F. Huang, *Journal of the American Chemical Society*, 2015, **137**, 10148-10151.